

Acoustic radiation force on thin elastic shells in liquid*

Run-Yang Mo(莫润阳), Jing Hu(胡静), Shi Chen(陈时), and Cheng-Hui Wang(王成会)[†]

Shaanxi Key Laboratory of Ultrasonics, School of Physics and Information Technology, Shaanxi Normal University, Xi'an 710119, China

(Received 6 March 2020; revised manuscript received 11 May 2020; accepted manuscript online 19 May 2020)

Based on the coupled acoustic scattering of two neighboring fluid-filled thin elastic shells suspending in an unbounded viscous liquid, an analytical method is developed to calculate the acoustic radiation force (ARF) of the shells. Two physical effects are taken into account: elastic radiation scattering and the multiple interactions of shells. Numerical results reveal that the magnitude of ARF can be enhanced by the sound radiation from the elastic shell undergoing forced vibrations and two resonant peaks can be observed on the ARF function curves. The feature of the lower peak is determined by the interactions and acoustic response of the back shell. The attractive forces can be obtained in the low kR_1 band for the case of radius ratio $R_2/R_1 > 1$, while the magnitude of ARF at the lower peak may be influenced to some extent by acoustic shielding phenomenon for the case of radius ratio $R_2/R_1 < 1$. Accordingly, the interactions of particles cannot be ignored. The results may provide a theoretical basis for precise manipulation of multiple particle systems.

Keywords: thin elastic shell, radiation force, elastic radiation scattering, mutual interactions

PACS: 43.25.+y, 43.35.+d

DOI: 10.1088/1674-1056/ab943e

1. Introduction

Researches have suggested the possibility of contact-free trapping or manipulating tiny sized objects (such as particles or biological cells) in a progressive acoustic wave.^[1–3] Particles suspended in acoustic fields are subjected to time-averaged forces from scattering of the acoustic waves, and these forces are named acoustic radiation force (ARF) theoretically.^[4] The problem of ARF on rigid and elastic particles has attracted much attention.^[5–9] Several theoretical models have been developed to calculate the ARF on objects in different types of acoustical fields.^[10–13] King proposed his formula of ARF on a rigid sphere,^[14] which could help us to estimate the absolute sound intensity by the radiation force method. However, Hasegawa and Yosioka^[15] found that King's theory deviated from the experimental values of the radiation force for spheres of brass, steel and stainless steel in the range of $ka > 2$ (a is the radius of the sphere, and k is the wavenumber in the liquid). Further, an improved ARF theory is developed by taking the elasticity of the solid sphere into account, and the results of the evaluation are in good agreement with the measurements.^[15]

The multiple features of the objects were considered in the investigations of acoustic radiation force, such as prolate spheroids, cylindrical particles, soft fluid spheres, and air bubbles.^[16–23] It is important to understand the radiation force related to the nonlinearity of sound propagation, and some potential applications could be extended. Objects could be pushed towards nodal or anti-nodal planes by radiation force in acoustic standing wave,^[16] and negative forces on spheres are found to be correlated with reduced acoustic

backscattering.^[13,17] The manipulation of pulsating spherical carrier^[10] has potential applications in drug delivery and the handling of the radiation force has proved feasible for spheres.

The scattering of floating objects submerged in liquid can give much information about the internal structure or compositions of materials, which is related to the multiple interaction between object and the surrounding medium.^[24,25] Usually, the object can be considered as solid particle or shell. For example, bacteria cells or spherical carriers were simplified as “shell model” to investigate the acoustic response.^[12,26] The acoustic radiation pressure on thin shell is different from that on solid sphere. Junger^[27] developed the theory of sound scattering of an acoustic plane wave by thin elastic shell submerged in liquid, and pointed out that the scattering pattern is the result of synthesis of rigid body scattering and elastic radiation scattering. Accordingly, the scattering effect could be enhanced by the sound radiation of the shell undergoing forced vibrations. The scattering of two elastic spherical shells in a boundless acoustic medium has been previously studied,^[28,29] and two physical reasons were proposed to explain the phenomenon that the function of total scattering is not in the form of the sum of the two individuals: multiple interactions between the two shells and the observed position of scattering wave. The first antisymmetric Lamb wave could be activated by the multiple interactions, and the enhancement band of the form function curve was observed.^[28] Therefore, it has been shown that the surface vibration modes play an important role in characterizing the sound backscattering.

While there have existed many publications on the interaction of acoustic waves with objects including researches focusing on arbitrary scattering and radiation force, the acous-

*Project supported by the National Natural Science Foundation of China (Grant Nos. 11974232, 11727813, 11474191, and 11474192).

[†]Corresponding author. E-mail: wangld001@snnu.edu.cn

tic dynamic behavior of thin elastic shell differs considerably from that of solid objects. According to the present sound scattering theories, we will explore the acoustic radiation force on thin elastic shells in an unbounded nonviscous liquid in this investigation. A simple mathematical model of two coupled thin shells is introduced, considering the effects of the surface deformation and mutual interactions of shells. This work expands the theories of acoustic radiation force, and conduces to a better understanding of the acoustic multi-interactions between different particles.

2. Coupled scattering of two elastic thin shells

We consider a pair of spherical shells with separation distance $D_{O_1O_2} = R_1 + R_2 + d$, where R_1 and R_2 are the radii of the two shells, respectively. The two shells are immersed in an unbounded liquid as shown in Fig. 1. The origins O_1 and O_2 of the two spherical coordinate systems $((r_j, \theta_j, (j = 1, 2)))$ are located at the centers of the left shell and right shell, respectively. The propagating direction of the incident plane wave is parallel to the z axis, and the wave is reflected and diffracted into and out of the shells. The mass density and sound speed of the fluid within and outside the shell are, respectively, (ρ, c) and (ρ_{in}, c_{in}) . The mass density of shell is denoted by ρ_s . We treat the acoustic radiation force on spherical shell by taking the thin shell approximation^[27] into account. This problem is based on the following assumptions: (i) the fluid medium satisfies the simplified wave equation; (ii) the material is isotropic, devoid of damping, and the deformation of the shell is subject to Hooke's law; (iii) the shell thickness is much less than other dimensions.

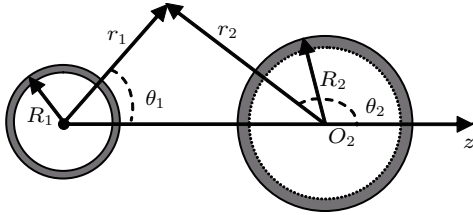


Fig. 1. Geometry of the model.

In the j -th local spherical coordinates $(j = 1, 2)$, the velocity potential of the incident wave and the outgoing waves scattered from the shells can be represented as follows:

$$\varphi_I^{(j)} = \varphi_0 \sum_{n=0}^{\infty} (2n+1) i^n j_n(kr_j) P_n \cos(\theta_j), \quad (1)$$

$$\varphi_s^{(j)} = \varphi_0 \sum_{n=0}^{\infty} (2n+1) i^n A_n^{(j)} h_n^{(2)}(kr_j) P_n \cos(\theta_j), \quad (2)$$

where $k = \omega/c$ with ω being the angular frequency, and c being the sound speed, $A_n^{(j)}$ are unknown expansion coefficients, φ_0 is the amplitude of velocity potential of the incident wave, $j_n(\cdot)$ and $h_n^{(2)}(\cdot)$ are the spherical Bessel function and Hankel

function of order n , and P_n is a Legendre polynomial. The time-dependent term $e^{i\omega t}$ is omitted in the expressions of the velocity potentials.

The total field is a result of the superposition of waves scattered on the surfaces of the system. Therefore, velocity potential around the shells in the surrounding liquid can be written as

$$\varphi_o^{(j)} = \varphi_0 \sum_{n=0}^{\infty} G_n^{(j)}(\omega) (2n+1) i^n P_n(\cos \theta_j), \quad (3)$$

where

$$G_n^{(j)} = \left(1 + \sum_{m=0}^{\infty} Q_{nm}^{(3-j)} \frac{2m+1}{2n+1} i^{m-n} A_m^{(3-j)} \right) j_n(kr_j) + A_n^{(j)} h_n^{(2)}(kr_j), \quad (4)$$

and the coefficients $A_n^{(j)}$ can be determined by the boundary conditions, the expression of $Q_{nm}^{(j)}$ was given in Appendix A.

The velocity potentials in the internal fluids of the shells are

$$\varphi_{in}^{(j)} = \varphi_0 \sum_{n=0}^{\infty} (2n+1) i^n B_n^{(j)} j_n(k_{in} r_j) P_n \cos(\theta_j), \quad (5)$$

where $B_n^{(j)}$ is the coefficient. The sound pressure of the outside liquid and inside liquid of the shells are obtained respectively, as follows:

$$p_o^{(j)} = i\omega\rho\varphi_o^{(j)}, \quad p_{in}^{(j)} = i\omega\rho_{in}\varphi_{in}^{(j)}. \quad (6)$$

The dynamic response of the shells is analyzed by mean of the standard method of the theory of mechanical vibration. In the spherical coordinates, the generalized radial and tangential displacement component related to the deformation of shell are given by two Fourier series^[27]

$$\delta = \sum_{n=0}^{\infty} a_{jn} P_n(\cos \theta_j), \quad (7)$$

$$\tau = - \sum_{n=0}^{\infty} b_{jn} P_n^1(\cos \theta_j), \quad (8)$$

where $P_n^1(x) = (1-x^2)^{1/2} dP_n(x)/dx$, and the coefficients a_{jn} and b_{jn} yield:

$$2R_j^2 h_j \rho_s \ddot{a}_{jn} + \frac{2Eh_j}{1-\nu} [2a_{jn} - (n+1)nb_{jn}] = -i\omega R_j^2 \bar{\varphi}_{jn}, \quad (9)$$

$$R_j^2 h_j \rho_s \ddot{b}_{jn} + \frac{Eh_j}{1-\nu} \left[-a_{jn} + \frac{n(n+1) - (1-\nu)}{1+\nu} b_{jn} \right] = 0. \quad (10)$$

Here

$$\begin{aligned} \bar{\varphi}_{jn} = & \rho (2n+1) i^n \left[j_n(x_j) + A_n^{(j)} h_n^{(2)}(x_j) \right. \\ & \left. + \sum_{m=0}^{\infty} Q_{nm}^{(3-j)} \frac{2m+1}{2n+1} i^{m-n} A_m^{(3-j)} j_n(x_j) \right] \\ & + \rho_i (2n+1) i^n B_n^{(j)} j_n(x_{ij}), \end{aligned}$$

and $x_j = kR_j$, $x_{ij} = k_i R_j$ ($k_i = \omega/c_{in}$ is the wavenumber of medium inside the shell), h_j is the thickness of the j -th shell, E and ν are the Young's modulus and Poisson's ratio of the shell medium. It should be noted that the model given by Eqs. (7)–(11) is limited to the condition of the non-dimensional thickness $h/R \ll 1$.^[27]

$$Z_{jn} = 2i \frac{h_j}{R_j} \left[\rho_s c x_j - \frac{E}{c x_j} \frac{(n-1)(n+2)E - 2\rho_s c^2 x_j^2 (1+\nu)}{[n(n+1) - (1-\nu)]E - \rho_s c^2 x_j^2 (1-\nu^2)} \right]. \quad (13)$$

The vibration of the shell is determined by the inner and outer sound fields, and the relation among $A_n^{(j)}$, $B_n^{(j)}$, and a_{jn} can be obtained from the boundary conditions. Accordingly, the continuity of normal velocity at the surface requires that

$$-\partial \varphi_o / \partial r_j |_{r_j=R_j} = -\partial \varphi_{in} / \partial r_j |_{r_j=R_j} = i \omega a_{jn}. \quad (14)$$

Substituting Eqs. (3), (5), and (11) into Eq. (14), one obtains

$$A_n^{(j)} = \alpha_n^{(j)} + i \beta_n^{(j)}, \quad (15)$$

$$B_n^{(j)} = \frac{c_{in}}{c j_n'(x_{ij})} \left[\left(1 + \sum_{m=0}^{\infty} \frac{2m+1}{2n+1} Q_{nm}^{(3-j)} i^{m-n} A_m^{(3-j)} \right) \times j_n'(x_j) + A_n^{(j)} h_n^{(2)}(x_j) \right], \quad (16)$$

where

$$\alpha_n^{(j)} = -\frac{1 + \delta_{1n}^{(j)} - \delta_{2n}^{(j)} \tan \gamma_n^{(j)}}{1 + (\tan \gamma_n^{(j)})^2},$$

$$\beta_n^{(j)} = -\frac{\delta_{2n}^{(j)} + \tan \gamma_n^{(j)} (1 + \delta_{1n}^{(j)})}{1 + (\tan \gamma_n^{(j)})^2},$$

$$\tan \gamma_n^{(j)} = \frac{n_n(x_j) + \bar{Z}_{jn} n_n'(x_j)}{j_n(x_j) + \bar{Z}_{jn} j_n'(x_j)},$$

$$\bar{Z}_{jn} = (\rho c)^{-1} \left[\rho_{in} c_{in} \frac{j_n(x_{ij})}{j_n'(x_{ij})} + i Z_{jn} \right],$$

$$\delta_{1n}^{(j)} = \text{Re} \left[\sum_{m=0}^{\infty} Q_{nm}^{(3-j)} \frac{2m+1}{2n+1} i^{m-n} A_m^{(3-j)} \right],$$

$$\delta_{2n}^{(j)} = \text{Im} \left[\sum_{m=0}^{\infty} Q_{nm}^{(3-j)} \frac{2m+1}{2n+1} i^{m-n} A_m^{(3-j)} \right].$$

Substituting Eq. (15) into Eq. (4) and setting $G_n^{(j)}(\omega) = V_n^{(j)} + i U_n^{(j)}$, one obtains

$$V_n^{(j)} = \text{Re}[G_n^{(j)}(\omega)] = \left(1 + \alpha_n^{(j)} + \delta_{1n}^{(j)} \right) j_n(kr_j) + \beta_n^{(j)} n_n(kr_j), \quad (17)$$

$$U_n^{(j)} = \text{Im}[G_n^{(j)}(\omega)] = \left(\delta_{2n}^{(j)} + \beta_n^{(j)} \right) j_n(kr_j) - \alpha_n^{(j)} n_n(kr_j), \quad (18)$$

where $n_n(\cdot)$ is the n -order spherical Bessel function of the second kind.

For the linearity problems, one has $\ddot{a}_{jn} = -\omega^2 a_{jn}$ and $\ddot{b}_{jn} = -\omega^2 b_{jn}$, and the solutions of a_{jn} and b_{jn} can be expressed as follows:

$$a_{jn} = -\varphi_0 \bar{\varphi}_{jn} / Z_{jn}, \quad (11)$$

$$b_{jn} = \frac{E}{1-\nu} \left[\frac{E}{1-\nu} \frac{n(n+1) - (1-\nu)}{1+\nu} - \rho_s c^2 x_j^2 \right]^{-1} a_{jn}, \quad (12)$$

3. Acoustic radiation force

The time averaged force acting on a spherical particle immersed in an infinite and ideal fluid is given by^[15]

$$\begin{aligned} \mathbf{F} = & - \left\langle \iint_{S_0} \rho (\mathbf{v}_r \mathbf{e}_r + \mathbf{v}_\theta \mathbf{e}_\theta) \mathbf{v}_r dS \right\rangle \\ & + \left\langle \iint_{S_0} \frac{\rho}{2} |\mathbf{v}|^2 \mathbf{e}_r dS \right\rangle \\ & - \left\langle \iint_{S_0} \frac{\rho}{2c^2} \left(\frac{\partial \psi}{\partial t} \right)^2 \mathbf{e}_r dS \right\rangle, \end{aligned} \quad (19)$$

where \mathbf{e}_r and \mathbf{e}_θ are radial and tangential components of the unit vector; radial and tangential components of the velocity vector \mathbf{v} are defined by $v_r = -\frac{\partial \psi}{\partial r}$ and $v_\theta = -\frac{1}{r} \frac{\partial \psi}{\partial \theta}$, where $\psi = \text{Re}[\varphi_0 e^{i\omega t}]$ is the real part of the total velocity potential in surrounding liquid; S_0 is the surface boundary at the equilibrium position; $dS = r \sin \theta dr d\theta$. The component in the x direction of the time averaged acoustic radiation force on the j -th shell in its local spherical coordinates can be broken down into four parts:

$$\langle F_{jx} \rangle = \langle F_r \rangle + \langle F_\theta \rangle + \langle F_{r\theta} \rangle + \langle F_t \rangle, \quad (20)$$

where

$$\begin{aligned} \langle F_r \rangle = & -2\pi\rho\varphi_0^2 x_j^2 \sum_{n=0}^{\infty} (n+1) \\ & \times \left(V_n^{(j)} U_{n+1}^{(j)} - U_n^{(j)} V_{n+1}^{(j)} \right)_{r_j=R_j}, \end{aligned}$$

$$\begin{aligned} \langle F_\theta \rangle = & 2\pi\rho\varphi_0^2 \sum_{n=0}^{\infty} n(n+1)(n+2) \\ & \times \left(V_n^{(j)} U_{n+1}^{(j)} - U_n^{(j)} V_{n+1}^{(j)} \right)_{r_j=R_j}, \end{aligned}$$

$$\begin{aligned} \langle F_{r\theta} \rangle = & 2\pi\rho\varphi_0^2 x_j \sum_{n=0}^{\infty} (n+1) \left[n \left(V_n^{(j)} U_{n+1}^{(j)} - U_n^{(j)} V_{n+1}^{(j)} \right) \right. \\ & \left. - (n+2) \left(V_n^{(j)} U_{n+1}^{(j)} - U_n^{(j)} V_{n+1}^{(j)} \right) \right]_{r_j=R_j}, \end{aligned}$$

$$\langle F_t \rangle = -2\pi\rho\varphi_0^2 x_j \sum_{n=0}^{\infty} (n+1) \left(V_n^{(j)} U_{n+1}^{(j)} - U_n^{(j)} V_{n+1}^{(j)} \right)_{r_j=R_j}.$$

Combining Eqs. (3), (12), (17), and (18) with Eq. (20) and making the integration over the outer surface of the j -th shell, the dimensionless radiation force function is obtained as

$$\begin{aligned}
 Yp_j &= \langle F_{jx} \rangle / (\bar{E}S_{jc}) \\
 &= \frac{4}{x_j^2} \sum_{n=0}^{\infty} \left\{ (n+1) \left(V_n^{(j)} U'_{n+1} - U_n^{(j)} V'_{n+1} \right) x_j^2 \right. \\
 &\quad - n(n+1)(n+2) \left(V_n^{(j)} U_{n+1}^{(j)} - U_n^{(j)} V_{n+1}^{(j)} \right) \\
 &\quad + x_j \left[n(n+1) \left(V_{n+1}^{(j)} U_n^{(j)} - U'_{n+1} V_n^{(j)} \right) \right. \\
 &\quad \left. \left. - (n+1)(n+2) \left(V_{n+1}^{(j)} U_n^{(j)} - U_{n+1} V_n^{(j)} \right) \right] \right. \\
 &\quad \left. + x_j^2 (n+1) \left(V_n^{(j)} U_{n+1}^{(j)} - U_n^{(j)} V_{n+1}^{(j)} \right) \right\}, \quad (21)
 \end{aligned}$$

where $\bar{E} = \frac{1}{2} \rho k^2 |\varphi_0|^2$ is the mean energy density of the incident plane wave, and $S_{jc} = \pi R_j^2$ is the cross-sectional of the object.

4. Numerical analysis

The acoustic radiation forces on coupled elastic shells in a plane wave field will be numerically studied in this section. The main objective here is to examine the effects related to the mutual interactions of the coupled scattering on the radiation force exerting on a thin elastic shell. Combining Eqs. (17) and (18) with Eqs. (20) and (21), the ARF function Yp_j ($j = 1, 2$) of the thin shells can be estimated. The results of the evaluation are illustrated in the case of stainless-steel shell, whose physical constants are cited from Ref. [15]. The surrounding liquid and inside medium are assumed to be water and air with properties of $\rho = 1000 \text{ kg/m}^3$ and $c = 1497 \text{ m/s}$ for water, and $\rho_{\text{in}} = 1.29 \text{ kg/m}^3$ and $c_{\text{in}} = 344 \text{ m/s}$ for air.

To check the validity of this model, the evaluations of the ARF function for a single thin shell, rigid sphere and elastic sphere are shown by the solid, broken and dashed curves in Fig. 2, respectively. King's formula^[14] and Hasegawa's formula^[15] are chosen for calculating the ARF function of rigid sphere and elastic sphere made of stainless steel, respectively. In our model, the thin shell has a thickness-to-radius ratio $h/R = 0.01$. The results show that Yp_1 begins at small value of kR_1 ($kR_1 < 0.5$), as though the thin shell is rigid. Deviation from the other curves appears with the increase of kR_1 ($kR_1 > 0.5$) and the Yp_1 arrives at a high resonant peak, which corresponds to the forced vibration of the thin shell activated by ultrasound sound wave. Because of the acoustic response of the thin elastic shell, the nonlinearity is enhanced, and Yp_1 of the thin elastic shell is larger than that of the sphere with the same size at the band of dynamics response of the thin shell when the objects are activated by the same sound wave. Comparing the curves of three models, one finds that each curve ascends in the range of $0 < kR_1 < \approx 1.6$. Therefore, the ARF function for the spherical bodies with the same outside radii

has similar physical properties related to the sound scattering. However, the sound scattering can be enhanced significantly by elastic radiation scattering^[27] of the thin elastic shell vibrated forcedly in the range $0.5 < kR_1 < \approx 5$. There are a number of sharp maxima and minima in the curve of solid elastic sphere, which results from the normal modes of the free vibration in the range of $kR_1 > \approx 1.6$.^[15] However, a similar phenomenon does not exist in the curve of the thin shell in that kR_1 range, which means the effects of the high-order normal modes of a thin shell on the ARF might be suppressed by other factors. Therefore, there is distinct deviation between the elastic shell and solid sphere.

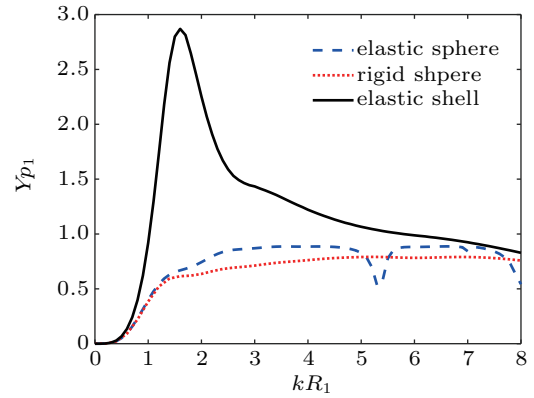


Fig. 2. Comparison among curves of ARF function Yp_1 versus kR_1 for different models: rigid/elastic sphere, single thin elastic shell.

In Fig. 3, all numerical results of the ARF function Yp_j ($j = 1$) are presented for the case of two identical stainless-steel shells ($R_1 = R_2$) with a thickness-to-radius ratio $h/R = 0.01$ and ratios of separation distance to radius $d/R_1 = 2, 2.5, 4, 10, 20, 50,$ and 100 , which are contrasted with those of a single shell for a range of $0 \leq kR_1 \leq 8$. At the very low kR_1 ($kR_1 < 1$), there is no distinctive difference among all the cases, which means that the nonlinear effects of interaction on ARF of shells can be omitted on condition that the wave length is much larger than the size of the shells. However, if the scattering system is approaching to acoustical resonance, the peaks of the ARF function are observed. As for a small separation of $d/R_1 = 2$ or 2.5 , there is a sharp resonant peak at $kR_1 \approx 1.3$, and ARF function fluctuates within the rough range of $2.8 < kR_1 < 6.0$, as shown in Fig. 3(a). The two shells are elastic scatters, and the radiation scattering influences the returned echoes extremely.^[27] The system is capable of pronounced resonant response in most modes. Therefore, when the two shells are very close to each other, the scattering are amplified by the interactions, and a sharp peak of Yp_1 is observed.

With a slightly larger separation $d/R_1 = 4$, two peaks are observed in the curve. Comparing the curve in the case $d/R_1 = 4$ with that of a single shell, the radiation force behind shell differs from that of the single only by a small deviation

in the range of $kR_1 > \approx 6.0$ as shown in Fig. 3(b). In the electromagnetic end-fire scattering case, this kind of small deviation has been explained as that the frontal shell could hide the back shell when acoustic wave frequency is higher than the resonant frequencies of the pair shells.^[28] With the increase in

the distance separation d , the interaction between the identical shells wakens. The ARF function Yp_1 approaches to that of the single when the separation- to-radius ratio $d/R_1 > 10$, and the multiple scattering effects of the shells can be neglected approximately.

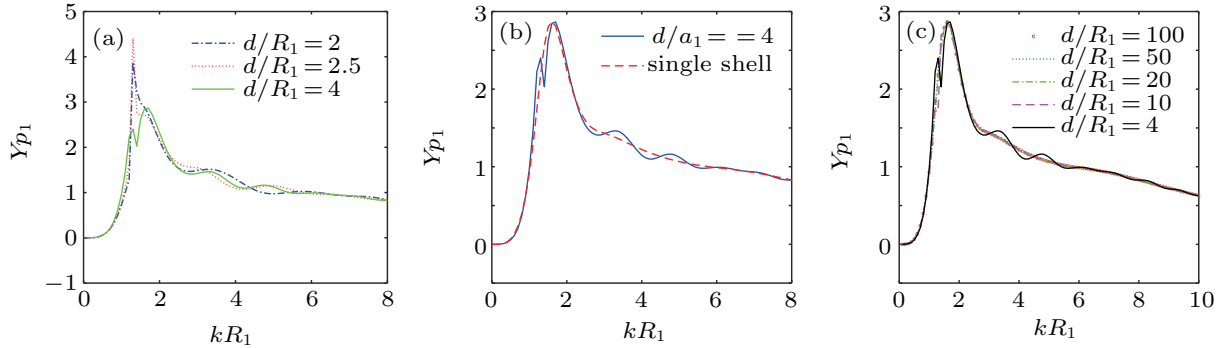


Fig. 3. Effects of separation distance on relation between ARF function Yp_1 and kR_1 for the frontal shell, showing comparison (a) among the cases $d/R_1 = 2, 2.5$, and 4 , (b) between the case $d/R_1 = 4$ and single shell, and (c) among $d/R_1 = 4, 10, 20, 50, 100$.

To fully understand the multiple interaction effects on the ARF of thin elastic shells, the dependence of the ARF function Yp_1 on the radii ratio ($R_2/R_1 = 0.5, 1, 2$, and 5) is shown in Fig. 4 for the cases of $d/R_1 = 4$ and $h/R = 0.01$. Figure 4(a) presents that the frontal shell can completely shield the back shell at the lower frequency band $kR_1 < 2.4$ for the case $R_2/R_1 = 0.5$, and the ARF of the frontal shell differs from the that of the single only by a small perturbation in the range $kR_1 > 2.6$. In each case for $d/R_1 = 4$, two peaks are observed, and the main peak is located at $kR_1 \approx 1.6$, while the lower (side) peaks for $R_2/R_1 = 0.5, 1, 2$, and 5 are situated at $2.6, 1.3, 0.7$ and 0.3 , respectively as shown in Figs. 4(b) and 4(c). Comparing the kR_1 values of the lower peaks for the case of

different radius ratios, one finds that the value of kR_1 is in reverse proportion to the size of the back shell approximately, which reveals that the lower peak might be related to the resonant response of the back shell to the driving acoustic wave. For the cases $R_2/R_1 > 1$, there exists a narrow kR_1 range in which the ARF is negative, and shells could be attracted to the sound source. According to the calculating results, for the case that the size of the back shell is larger than that of the frontal, its back-scattering is stronger than that of the frontal, which enhances the multiple interaction effects on ARF of the frontal. Therefore, the ARF can be significantly affected by the multiple interactions between shells in the resonant region of the acoustic response of the pair.

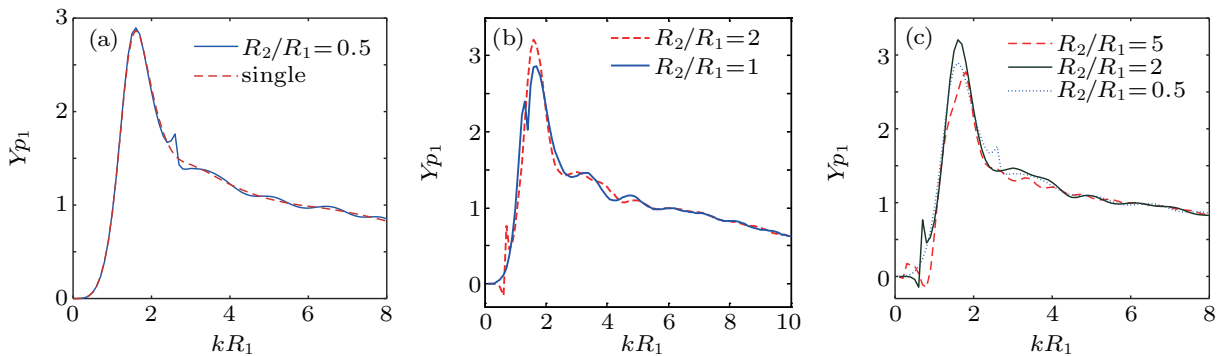


Fig. 4. Effects of radius ratio on relation between ARF function Yp_1 and kR_1 for frontal shell, showing (a) comparison among the case $R_2/R_1 = 1$ and single shell, (b) between the cases $R_2/R_1 = 1, 2$, and (c) between the cases $R_2/R_1 = 0.5, 2, 5$.

To further check the validity, the effects of the shell thickness on the ARF are investigated numerically as shown in Fig. 5. The magnitude of the main peak in ARF function Yp_1 curve decreases with the increase of the shell thickness at the kR_1 band of resonant response to incident progressive wave when $R_2/R_1 = 1$ and $d/R_1 = 4$. Elastic scattering of a thin shell^[27] is the important reason for the difference between the scattering action of thin shell and that of a solid elastic body.

The acoustic scattering feature of the thick shells is different from that of thin shells, and the elastic waves (transverse wave and longitudinal wave) might be activated in the medium of a thick shell, which relates to the surface vibration (or wave) of the thin elastic shell. Therefore, this model should be limited to the application to predicting the ARF of the thin elastic shell precisely, *i.e.*, shelled medical carrier, micro-capsular ultrasound contrast agent.

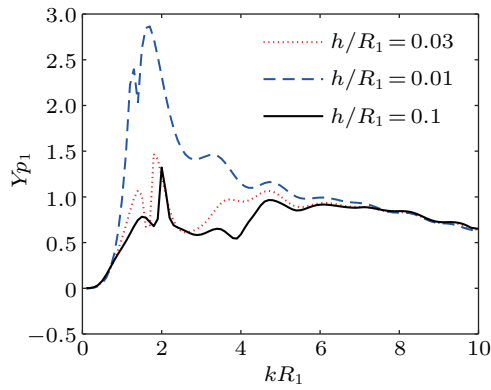


Fig. 5. Effect of shell thickness on relation between ARF function Y_{p1} and kR_1 for frontal shell.

5. Conclusions

This theory is based on the thin elastic shell approximation, and it may be considered as a development of the ARF theory, including the elastic radiation of thin shells and the mutual interactions of multiple particle systems.

Based on the rectified model of sound scattering of a thin elastic shell pair including the effects of elastic scattering of the shell and interaction between shells, the acoustic radiation force of a thin elastic shell suspended in a plane progressive sound wave field is calculated approximately. Due to the non-linear nature of the acoustic radiation, some new features related to the multiple interactions of two shells in liquid are highlighted. Enhanced resonant peak in the curve of ARF force versus kR_1 results from elastic scattering. The interactions between shells is closely related to the identify character of acoustic radiation force, and the negative force is obtained at the band related to the resonant response of the back shell. Acoustic shielding phenomenon of the frontal shell first impinged upon by the incident wave can affect the ARF magnitude of lower peak to some extent for the case $R_2/R_1 < 1$. The kR_1 value related to the lower peak is in reverse proportion to the size of the back shell approximately. Therefore, the acoustic resonant response of thin shells should be emphasized for the manipulation of multiple particle systems.

Appendix A

The expression of $Q_{nm}^{(j)}$ is given as follows:^[30]

$$Q_{nm}^{(j)} = \sum_{\alpha=|n-m|}^{n+m} (-1)^{\alpha(j-1)} (2\alpha+1) (-i)^{\alpha} S_n^{m\alpha} h_{\alpha}^{(2)}(kD), \tag{A1}$$

where $S_n^{m\alpha} = (m\alpha 00|n0)^2$, Clebsch–Gordan coefficient is defined with using $q = (\alpha + m + n)/2$ and $2q$ is even, as^[31]

$$(m\alpha 00|n0) = \frac{(-1)^{n+q} q!}{(q-n)!(q-m)!(q-\alpha)!} \times \sqrt{\frac{2n+1}{(2q+1)!} (2q-2n)!(2q-2m)!(2q-2\alpha)!}, \tag{A2}$$

and when $2q$ is odd, as $(m\alpha 00|n0) = 0$.

References

- [1] Mohapatra A R, Sepehrirahnama S and Lim K 2018 *Phys. Rev. E* **97** 053105
- [2] Yu H, Yao J, Wu D, Wu X and Liu X 2018 *Phys. Rev. E* **98** 053105
- [3] Baresch D, Thomas J L and Marchiano R 2016 *Phys. Rev. Lett.* **116** 024301
- [4] Mikkel Settnes and Henrik Bruus 2012 *Phys. Rev. E* **85** 016327
- [5] Hasagawa T 1979 *J. Acoust. Soc. Am.* **65** 32
- [6] Xie W J and Wei B 2004 *Phys. Rev. E* **70** 046611
- [7] Zang Y C, Qiao Y P, Liu J H and Liu X Z 2019 *Chin. Phys. B* **28** 034301
- [8] Gao S, Mao Y W, Liu J H and Liu X Z 2018 *Chin. Phys. B* **27** 014302
- [9] Wu Y R and Wang C H 2017 *Chin. Phys. B* **26** 114303
- [10] Majid Rajabi and Alireza Mojahed 2018 *Ultrasonics* **83** 146
- [11] Mahdi Azarpeyvand and Mohannad Azarpeyvand 2013 *J. Sound Vib.* **332** 2338
- [12] Mitri F G 2017 *Ultrasonics* **74** 62
- [13] Zhang Likun and Marston Philip L 2011 *Phys. Rev. E* **84** 035601(R)
- [14] King L V 1934 *Proc. Roy. Soc. A* **137** 212
- [15] Hasegawa Takahi and Yosioka Katuya 1969 *J. Acous. Soc. Am.* **46** 1139
- [16] Mitri F G 2005 *Physica D* **212** 66
- [17] Marston P L 2006 *J. Acous. Soc. Am.* **120** 3518
- [18] Walker W F 1999 *J. Acous. Soc. Am.* **105** 2508
- [19] Baresch Diego, Thomas Jean-Louis and Marchiano Régis 2013 *J. Acous. Soc. Am.* **133** 25
- [20] Glauber T S 2014 *J. Acous. Soc. Am.* **136** 2405
- [21] Zhang L K and Marston P L 2014 *J. Acous. Soc. Am.* **136** 2917
- [22] Ghanem M A, Maxwell A D, Sapozhnikov O A, Khokhlova V A and Bailey M R 2019 *Phys. Rev. Appl.* **12** 044076
- [23] Leão-Neto J P, Lopes J H and Silva G T 2016 *Phys. Rev. Appl.* **6** 024025
- [24] Sammelmann G S, Trivett D H and Hackman R H 1989 *J. Acous. Soc. Am.* **85** 114
- [25] Goodman R R 1962 *J. Acous. Soc. Am.* **34** 338
- [26] Zinin P V, Allen I I J S and Levin V M 2005 *Phys. Rev. E* **72** 061907
- [27] Junger M C 1952 *J. Acous. Soc. Am.* **24** 366
- [28] Huang H and Gaunard G C 1997 *J. Acous. Soc. Am.* **101** 2659
- [29] Simon G, Pailhas Y, Andrade M A B, Reboud J, Marque-Hueso J, Desmullies M P Y, Cooper J M, Riehle M O and Bernassau A L 2018 *Appl. Phys. Lett.* **113** 044101
- [30] Wang C and Cheng J 2013 *J. Acous. Soc. Am.* **134** 1675
- [31] Hasheminejad S M and Azarpeyvand M 2004 *Ocean Eng.* **31** 1129